

A Space-Time Coded Mills Cross MIMO Architecture to Improve DOA Estimation and Its Performance Evaluation by Field Experiments

CAHİT UĞUR UNGAN 

ÇAĞATAY CANDAN 

TOLGA CILOGLU 

Middle East Technical University, Ankara, Turkey

Conventional Mills Cross architecture suffers from poor direction-of-arrival angle estimation accuracy in the dimension that the transmitter is aligned. To improve the estimation accuracy, a space-time coded, multiple-input multiple-output (MIMO) direction finding method, with complementary codes is presented. The performance of the suggested MIMO Mills Cross architecture has been evaluated by underwater field experiments. Field experiments confirm the feasibility of the proposed approach and illustrate the performance gains. Since the proposed approach does not require any changes in the conventional Mills Cross hardware, the performance improvement can also be realized by a software reconfiguration for existing legacy systems.

I. INTRODUCTION

Mills Cross [1] is a well-known, low-complexity array structure utilized in sonar and radar applications. In underwater applications, the architecture is composed of two linear transducer arrays; a transmitter array of projectors and a receiver array of hydrophones. If these two arrays are perpendicular to each other, the beam pattern, by the product theorem, is the same as that of a planar rectangular array of transducers of the same overall dimensions [2]. Moreover, in [3] it is shown that the power pattern of a conventional planar array can be obtained by multiplicative T-arrays and Mills Cross structures. Therefore, the Mills Cross technique is a convenient choice for light weight and cost effective underwater applications. Multibeam echo sounders, [4]–[6], and forward looking sonars, [7], [8], are some examples of such Mills Cross applications.

Direction-of-arrival (DOA) estimation with the standard Mills Cross architecture is based on conventional beam-forming techniques. In the forward looking case, to detect objects like mines and obstacles, the conventional way is to ensonify a discrete set of elevation angles consecutively (i.e., consecutive horizontal strips) with a vertical transmitter array. Then, for each horizontal strip so formed, angle of arrival in azimuth is determined by conventional beamforming methods with a horizontal receiver array. This method is summarized in Fig. 1. A drawback is the limitation of the accuracy of estimated elevation angles by the amount of angular displacement between the consecutive horizontal strips. For the conventional Mills Cross technique it is also possible to utilize super-resolution techniques to obtain a finer estimate in azimuth angle with the available horizontal receiver array. However, with fixed transmit beam directions such an option is not available for elevation angles, since a vertical receiver array that can search in elevation on reception is not present. In this article, we show that by using multiple-input multiple-output (MIMO) radar/sonar techniques, the accuracy of elevation angle estimates can be improved when searching for a target in a three-dimensional (3-D) volume with a forward looking Mills Cross architecture having a horizontal receiver array.

In the radar literature, two basic operation types for MIMO systems are defined. In the first one, which is sometimes referred to as statistical MIMO radar, transmit and receive elements are positioned far away from each other to obtain independent scattering responses for each transmit and receive pair [9]. In the second type, which is called coherent MIMO radar, transmit and receive elements are closely spaced so that the target in the far field is seen at the same spatial angle by the whole system [10]. For the latter type, which is under our consideration for DOA estimation purposes, one needs to investigate the differences of the MIMO radar concept with phased array systems. In phased arrays, a single waveform is transmitted through different antenna elements with different phase lags, so the waveforms at different elements are perfectly correlated. On the other hand, for the MIMO case, the transmit array elements emit orthogonal or uncorrelated waveforms. As a

Manuscript received January 13, 2016; revised June 25, 2018; released for publication July 30, 2019. Date of publication November 8, 2019; date of current version June 9, 2020.

DOI. No. 10.1109/TAES.2019.2952480

Refereeing of this contribution was handled by K. Davidson.

Authors' addresses: C. U. Uungan is with the Department of Electrical and Electronics Engineering, Middle East Technical University, Ankara 06800, Turkey, E-mail: (cuungan@hotmail.com); Ç. Candan and T. Ciloglu are with the Middle East Technical University, Ankara 06800, Turkey, E-mail: (ccandan@metu.edu.tr; ciltolga@metu.edu.tr). (*Corresponding author: Cahit Uğur Uungan.*)

0018-9251 © 2019 IEEE

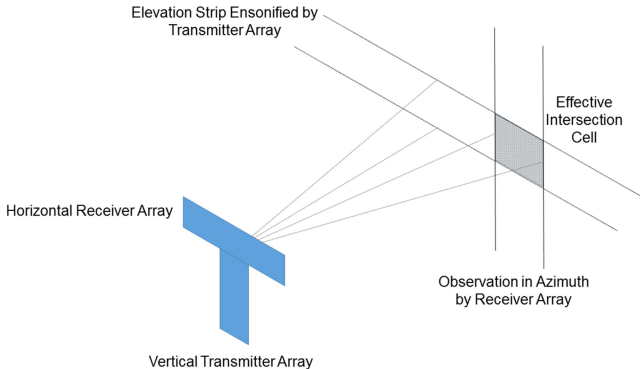


Fig. 1. Mills Cross architecture to perform a 2-D search with two perpendicular linear arrays.

result, the degrees of freedom to design transmit and receive beamformers is increased. Additional degrees of freedom can be used to optimize a desired performance criterion as stated in [11]. In [11], possible improvements are described as enhancing detectability, increasing clutter or interference rejection, improving the quality of the estimated radar map, improving spatial resolution, or reducing search time by using MIMO structure.

The sonar community has also expressed similar interest in utilizing the statistical and coherent MIMO radar concepts in underwater applications [12]–[18]. In [17] and [18], the authors compare coherent MIMO techniques with the classical phased array structure. The results show significant improvements on DOA estimates when MIMO techniques are used.

In the literature, the main drawback of the coherent MIMO radar/sonar concept is indicated as the SNR loss since the transmitted pulses are no longer correlated and cannot be added up constructively. One solution to this problem is to extend the duration of the pulses to compensate for the SNR loss since the decrease in the search time enables such a modification [19]. The other popular method is a hybrid approach that combines the MIMO radar/sonar concept with conventional-phased array methods by using subarrays [20]–[22]. In the hybrid approach, the whole array is partitioned into subarrays. Transmitted waveforms are orthogonal or uncorrelated across subarrays. On the other hand, the elements of a subarray transmit the phase shifted replicas of the same waveform to achieve the directivity gain. As a result, a tradeoff between the advantages of two architectures becomes possible. Moreover, it is often impractical to use the whole array as a MIMO array since, as the number of MIMO elements increases, a larger set of waveforms with autocorrelation and crosscorrelation functions constrained to satisfy ideal orthogonality conditions is needed. Suboptimum solutions such as using Gold sequences and nonoverlapping signals in frequency spectrum to overcome this challenge are suggested [23], [24]. A comprehensive literature survey of radar waveform design can be found in [25]. Another attractive solution that does not require partitioning the total bandwidth among the subarrays is using space-time coding to achieve the orthogonality

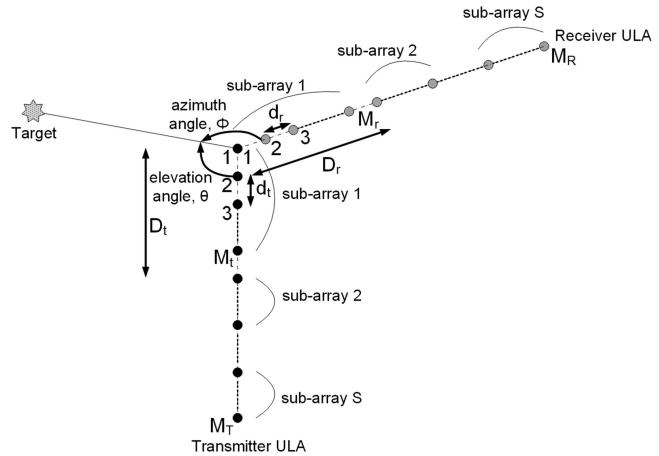


Fig. 2. Two perpendicular ULAs to search for a target in 3-D coordinates.

requirements of the MIMO radar/sonar system. A specific space-time coding approach through complementary codes, also known as Golay complementary sequences [26], have attracted a growing interest due to their exact orthogonality properties when used in pairs [27], [28]. The usage of complementary codes along with the MIMO radar/sonar architecture is proposed in [29]. This concept is discussed in detail in Section IV.

In this article, our aim is to develop a novel approach to obtaining a cost effective and accurate sonar system for obstacle detection from a slowly moving platform. Although the complementary pair waveforms are vulnerable to Doppler effects as indicated in [28], the evaluation of a Mills Cross type sonar system utilizing the hybrid approach by transmitting Golay complementary waveforms for such a DOA estimation application seems to be worthwhile. The structure is described in detail in Section II. The practical performance of the suggested structure is verified by the field experiments described in Section V.

Throughout this article, we adopt the following notation: lowercase letters with bars denote column vectors, whereas boldface capital letters denote matrices. The transpose, the conjugate, and the Hermitian (i.e., the conjugate transpose) operators are denoted by the symbols $(\cdot)^T$, $(\cdot)^*$, and $(\cdot)^H$, respectively. The symbols used throughout this article are summarized in Table I for quick reference.

II. SIGNAL MODEL FOR MIMO MILLS CROSS ARCHITECTURE

The Mills Cross architecture is composed of a uniform linear array of M_T transmitter elements and a uniform linear array of M_R receiver elements where the transmitter and the receiver arrays are perpendicular to each other. Additionally, we assume that the overall array is looking forward to ensonify the elevation angles with a vertical transmitter array and to estimate the azimuth angles of a possible target with a horizontal receiver array. Such a configuration is shown in Fig. 2. In this configuration, the phase references of the uniform linear arrays are assumed to be the first

TABLE I
Summary of the Symbols

Symbol	Description
M_T, M_R	The number of transmit/receive elements of the system
M_t, M_r	The number of transmit/receive elements in each sub-array
S	The number of orthogonal signals (also the number of sub-arrays)
D_t, D_r	The distance between the phase centers of the transmit/receive sub-arrays
d_t, d_r	The inter element distance in the transmit/receive sub-arrays
θ_t, ϕ_t	Elevation and azimuth angle of the target, respectively
θ_0, ϕ_0	Ensonified elevation angle and steered azimuth angle at the receiver, respectively
$\bar{a}_t(\theta)$	Transmit sub-array steering vector for an elevation angle
$\bar{a}_r(\phi)$	Array steering vector for a receiver sub-array
$\bar{a}_T(\theta)$	Array steering vector for the elevation angle θ when the sub-arrays are considered as single transmitting structures
$\bar{a}_R(\phi)$	Array steering vector on reception when the sub-arrays are considered as single transmitting structures
$\mathbf{A}(\phi, \theta)$	2-D steering matrix corresponding to the 2-D virtual array
$s_i(t)$	Signal transmitted by the i^{th} transmitter sub-array
$s_{\theta, i}(t)$	Signal due to the i^{th} transmitter sub-array at the target elevation
$\bar{x}(t)$	Received signal vector when the sub-arrays are considered as single transmitting structures
$\bar{y}_i(t)$	Received signal vector of the i^{th} receiver sub-array
$y_{i, \phi_0}(t)$	Received signal for the i^{th} receiver sub-array after beamforming
$y_{i, k}$	The peak output of the k^{th} matched filter (corresponding to the k^{th} transmitted signal) of the i^{th} receiver sub-array
\mathbf{Y}	The matched filter peak output matrix corresponding to the 2-D virtual array
$\mathbf{E}_{2 \times 2}$	Transmitted signal matrix representing the signals from 2 sub-arrays for 2 successive PRIs
\mathbf{H}	Channel response matrix whose ij^{th} element h_{ij} represents the channel response from the i^{th} transmitting sub-array to the j^{th} receiving sub-array
\mathbf{R}	Receive matrix whose rows represent the receiving sub-arrays, and columns represent the successive PRIs

elements. Moreover, the phase references of the transmitter and receiver arrays are assumed to coincide for the sake of simplicity of the derivations.

To be able to utilize MIMO radar/sonar techniques, we will partition the transmitter and receiver arrays into subarrays. When the array is in the transmission mode, all elements of a transmit subarray emit coherent signals to maximize the power at the intended elevation angle, whereas signals of different subarrays are orthogonal or uncorrelated. In the receiving mode, the outputs of the elements of a receiver subarray are spatially filtered (i.e., beamforming) to detect a possible echo at the intended azimuth angle. Moreover, each receive subarray is considered as a single receiver unit which contains filters matched to the transmitted signals to obtain the MIMO radar/sonar structure, [19]. In [19], it is shown that the sufficient statistics vector, which actually contains the outputs of the matched filters that filters the incoming signals with respect to all of the transmitted signals at each receiver element, can be used to estimate the parameters such as target angles in azimuth and elevation. In Fig. 3, the receiver structure of [19] is shown with a slight modification.

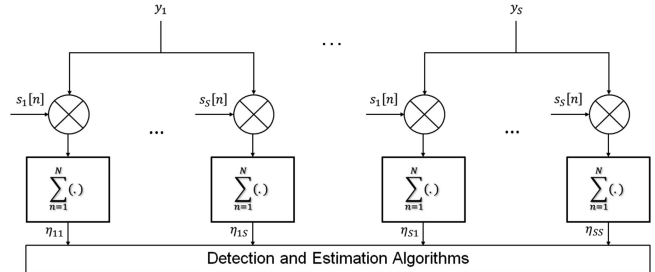


Fig. 3. Receiver architecture proposed in [19] with a slight modification.

Assuming narrowband and far field conditions are satisfied, let us now consider S orthogonal signals to be transmitted from the transmitter array, such as $s_i(t)$ where $i = 1, 2, \dots, S$. The transmitter and receiver arrays are partitioned into S nonoverlapping identical subarrays for the proposed architecture. Hence, we may define the number of elements in transmitter and receiver subarrays as M_t and M_r , which are equal to M_T/S and M_R/S consecutively. According to Fig. 2, to maximize the transmitted power at a given elevation angle, θ_0 (according to the given convention), the signals emitted from the omnidirectional elements of a subarray should be weighted with the appropriate vector, \bar{w} given as

$$\bar{w} = [1 e^{-j(2\pi f d_t \cos \theta_0 / c)} \dots e^{-j(M_t-1)(2\pi f d_t \cos \theta_0 / c)}]^T.$$

Here, f is the operating frequency of the array, d_t is the inter element distance in the transmit subarray, and c is the speed of sound. Note that the required weight vector is actually the conjugate of the transmit subarray steering vector, $\bar{a}_t(\theta_0)$, for the direction θ_0 . Thus, when the i^{th} transmit subarray directs its signals at the elevation angle θ_0 , the total signal due to the corresponding subarray in front of a target positioned at θ_t degrees in elevation becomes

$$s_{\theta, i}(t) = \bar{a}_t^T(\theta_t) \bar{a}_t^*(\theta_0) s_i(t). \quad (1)$$

In the above equation, $\bar{a}(\theta)$ is the array steering vector and equals to $[1 e^{j(2\pi f d_t \cos \theta) / c} \dots e^{j(M_t-1)(2\pi f d_t \cos \theta) / c}]^T$ where $\bar{a}^*(\theta)$ represents the conjugate of the steering vector. We can clearly see that when the target is at the center of the transmit beam (i.e., $\theta_0 = \theta_t$), $s_{\theta, i}(t) = M_t s_i(t)$ and the signal power at target location is maximized.

Now, let us consider the transmit subarrays as single transmitter elements and express the overall signal for a target positioned at a given elevation angle of θ_t . This time the transmit array steering vector, $\bar{a}_T(\theta_t)$, can be written as

$$\bar{a}_T(\theta_t) = [1 e^{-j(2\pi f D_t \cos \theta_t) / c} \dots e^{-j(S-1)(2\pi f D_t \cos \theta_t) / c}]^T.$$

Here, D_t is the distance between the phase centers of the transmit subarrays (i.e., the distance between the first elements of the subarrays in our model). Therefore, the total signal due to all transmit subarrays in front of a target at elevation angle θ_t becomes

$$s_{\theta, \text{TOT}}(t) = \bar{a}_T^T(\theta_t) \bar{s}_\theta(t). \quad (2)$$

In the above equation, $\bar{s}_\theta(t)$ is the signal vector containing S orthogonal signals emitted from the subarrays

$$\bar{s}_\theta(t) = [s_{\theta,1}(t) \dots s_{\theta,S}(t)]^T.$$

In a similar fashion, the receiver array is partitioned into S receiver subarrays for the MIMO Mills Cross architecture. The receiver subarrays are all steered to a particular azimuth angle, ϕ_0 , and the target is assumed to be at the azimuth angle, ϕ_t . First, we consider all the receiver subarrays as independent receiving elements and write the received signal vector, $\bar{x}(t)$, at these elements as

$$\bar{x}(t) = \alpha \bar{a}_R(\phi_t) s_{\theta,\text{TOT}}(t). \quad (3)$$

In (3), we omit the noise term, for now, to simplify the description. Here, α is the complex coefficient that includes both the target strength and some potential phase errors like the one due to the lack of perfect synchronization between the receiver and the transmitter. Additionally, $\bar{a}_R(\phi_t)$ is the receive steering vector when the subarrays are considered as independent receiving elements and it can be written as

$$\bar{a}_R(\phi_t) = [1 e^{j(2\pi f D_r \cos \phi_t)/c} \dots e^{j(S-1)(2\pi f D_r \cos \phi_t)/c}]^T. \quad (4)$$

The constant D_r indicates the distance between the phase centers of the receive subarrays (i.e., the distance between the first elements of the subarrays in our model). Now, if we consider the i th receive subarray, we can write the received signal vector, $\bar{y}_i(t)$, of this subarray as

$$\bar{y}_i(t) = \alpha \bar{a}_r(\phi_t) a_{R,i}(\phi_t) s_{\theta,\text{TOT}}(t)$$

with $a_{R,i}(\phi_t)$ is the i th element of the steering vector defined in (4) and $\bar{a}_r(\phi_t)$ is the receive steering vector of a receiver subarray in the MIMO Mills Cross architecture. For the receiving case, we emphasize again that all the receiver subarrays are forming beams for a particular azimuth angle, ϕ_0 , and the i th receive subarray produces the signal $y_{i,\phi_0}(t)$ given as

$$\begin{aligned} y_{i,\phi_0}(t) &= \bar{a}_r^H(\phi_0) \bar{y}_i(t) \\ &= \alpha \bar{a}_r^H(\phi_0) \bar{a}_r(\phi_t) a_{R,i}(\phi_t) s_{\theta,\text{TOT}}(t). \end{aligned} \quad (5)$$

In (5), $\bar{a}_r^H(\phi_0)$ represents the coefficients of the spatial filter to maximize the input arriving at the azimuth angle ϕ_0 , which is the Hermitian of the array steering vector for the direction ϕ_0 . After beamforming, in order to reap the benefit of MIMO radar/sonar concept, the beamformed output should be filtered by the matched filters for each transmitted orthogonal signal. Recalling the orthogonality condition

$$\int_0^T s_i(t) s_j(t) dt = \begin{cases} E_s, & \text{if } i = j \\ 0, & \text{otherwise.} \end{cases}$$

where E_s is the energy of the signal and T is the pulse duration. The peak output sampled at the appropriate time instant at the k th matched filter of the i th subarray can be written, by putting (1) and (2) into (5), as

$$y_{i,k} = \alpha a_{R,i}(\phi_t) \bar{a}_r^H(\phi_0) \bar{a}_r(\phi_t) a_{T,k}(\theta_t) \bar{a}_T^T(\theta_t) \bar{a}_T^*(\theta_0) E_s. \quad (6)$$

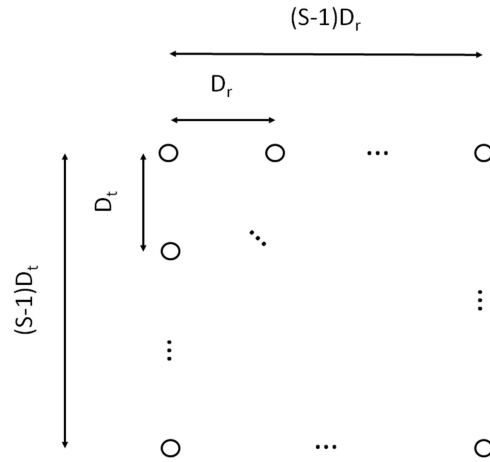


Fig. 4. Virtual 2-D array produced by MIMO Mills Cross architecture according to $\mathbf{A}^T(\phi, \theta)$.

Now let us define

$$\begin{aligned} \beta_r &\triangleq \bar{a}_r^H(\phi_0) \bar{a}_r(\phi_t) \\ \beta_t &\triangleq \bar{a}_T^T(\theta_t) \bar{a}_T^*(\theta_0) \end{aligned}$$

as the complex coefficients due to the mismatch between the exact target position and the subarray steering directions in azimuth and elevation angles, respectively. Then, (6) becomes

$$y_{i,k} = \alpha \beta_r \beta_t E_s a_{R,i}(\phi_t) a_{T,k}(\theta_t) \quad (7)$$

with the assumption of identical signal energy of E_s for different pulses. In (7), $a_{R,i}(\phi_t)$ is the contribution of the i th receiver subarray to the receiver steering vector structure when the subarrays are considered as single elements and $a_{T,k}(\theta_t)$ is the contribution of the k th transmitter subarray to the transmitter steering vector when the subarrays are considered as single elements. Thus, we can form an $S \times S$ matched filter output matrix, \mathbf{Y} , composed of all possible values of i and k , where $i = 1, 2, \dots, S$ and $k = 1, 2, \dots, S$.

$$\mathbf{Y} = \alpha \beta_r \beta_t E_s \bar{a}_R(\phi_t) \bar{a}_T^T(\theta_t).$$

Now, we can define a new steering $S \times S$ matrix of $\mathbf{A}(\phi, \theta)$ for the virtual array as

$$\mathbf{A}(\phi, \theta) \triangleq \bar{a}_R(\phi) \bar{a}_T^T(\theta).$$

In effect, we construct a virtual 2-D rectangular array composed of S^2 elements as shown in Fig. 4 that we can use to perform a search algorithm on the received data to estimate the elevation angle with higher accuracy. More specifically, assuming a Mills Cross system that can switch back and forth between conventional and suggested MIMO modes, the target detection can take place using the conventional structure and once the target is detected, the system can switch to MIMO mode to generate higher accuracy estimates for the azimuth and elevation angles.

Up to this point, we have assumed the availability of the perfectly orthogonal transmitted signals. For a practical MIMO sonar system, we should expect that each transmitted signal can be received with different time delays

due to multipaths, multiple targets on arbitrary locations, etc. Hence, the autocorrelation functions of the transmitted signals should have a peak at zero delay and be equal to zero elsewhere. Moreover, the cross correlations of the transmitted signals should be equal to zero for any time delay. When these conditions are met, a MIMO radar/sonar system achieves its full performance. However, in practice it is very difficult to satisfy these conditions. In Section III, we still assume perfect orthogonality but include the additive noise term in the model so as to study the performance improvement of the suggested MIMO Mills Cross system. In the following section, we present a space-time coding scheme to obtain orthogonality on successive pulse repetition intervals (PRIs).

III. CRAMER-RAO LOWER BOUND FOR THE MIMO ARCHITECTURE

So far, we have omitted the noise component throughout the derivations. Now, we derive the observation model to evaluate the performance of the MIMO Mills Cross architecture for elevation angle estimation. The observation vector, \bar{r} , for the elevation angle estimation can be written as

$$\bar{r} = \text{vec}(\mathbf{Y}) + \bar{\omega}.$$

Here, $\text{vec}(\mathbf{Y})$ is an $S^2 \times 1$ column vector obtained by vertically ordering the columns of the matched filter output matrix, \mathbf{Y} and $\bar{\omega}$ is the noise vector having independent identically distributed white Gaussian components. With this observation model, we can derive the Cramer-Rao Lower Bound (CRLB) for the elevation angle estimation assuming the azimuth angle is perfectly known. The Fisher information, $I(\theta)$, for such a case is defined as, [30]

$$I(\theta) = 2\Re \left\{ \frac{\partial \bar{y}^H}{\partial \theta} \mathbf{C}_{\bar{r}}^{-1} \frac{\partial \bar{y}}{\partial \theta} \right\}$$

$$\bar{y} = \text{vec}(\mathbf{Y}).$$

Here, $\mathbf{C}_{\bar{r}}^{-1}$ is the inverse of the covariance matrix of the observation vector; $\mathbf{C}_{\bar{r}}^{-1} = (1/(\sigma_{\omega}^2))\mathbf{I}$, where σ_{ω}^2 is the variance of the additive white Gaussian noise and \mathbf{I} is the identity matrix of size $S^2 \times S^2$. Having obtained the Fisher information, the CRLB is

$$\text{CRLB}_{\theta} = \frac{1}{I(\theta)}.$$

Now, let us assume, a Mills Cross architecture with 20 transmitter and 24 receiver elements with interelement distances, $d_t = d_r = \lambda/2$. We also assume that a target is positioned at a 0.5 degree offset with the boresight of the transmitter subarrays. With these assumptions, the CRLB for the standard deviation of the elevation angle estimation errors with respect to SNR, where the number of orthogonal signals, S , is set to 2, is plotted in Fig. 5. This specific Mills Cross setup for which the numerical values of the CRLB is calculated is also the setup for which the underwater field tests described in Section V are carried out.

Comparisons with the conventional system are as follows: for a uniformly illuminated rectangular antenna, the

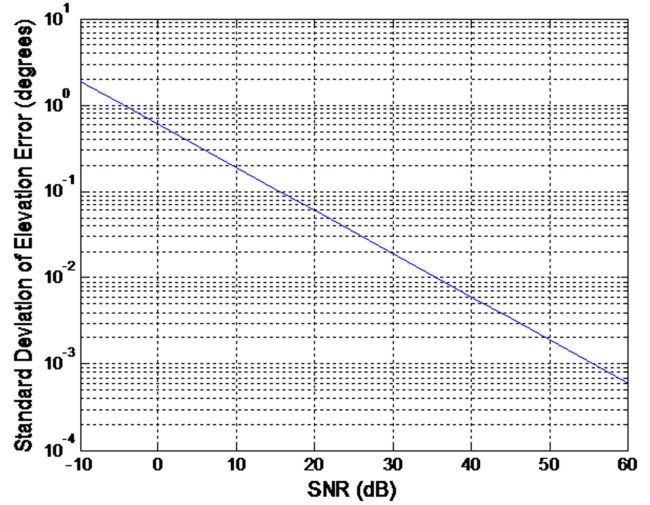


Fig. 5. Standard deviation of the error with respect to SNR.

3-dB beamwidth (in one dimension) is given in [31] as

$$3\text{-dB beamwidth} = 2 \sin^{-1} \left(\frac{1.4\lambda}{\pi D} \right) \approx 0.89 \frac{\lambda}{D}$$

where D is the aperture size of the array. Hence, we can say that a uniform linear array (ULA) having 20 elements with the interelement spacing of $\lambda/2$, the 3-dB beamwidth is approximately 0.089 radians or 5.1 degrees. For such an array with a conventional Mills Cross architecture, we may expect that the sonar system uses fixed predefined transmit beams separated by this 3-dB beamwidth to search for a target in a 3-D volume. For a small enough target, we may assume that the target will be detected by only one transmit beam and the elevation angle that corresponds to the transmit beam center is assumed as the elevation angle of the target. For instance, 5.1 degrees of beamwidth corresponds to nearly 9 at 100 m distance when the target is close to the boresight in elevation. If the target under concern is a sea mine with a diameter less than a few meters, such a scenario is practical. When the range increases, for smaller beamwidths such an assumption may still be valid. Therefore, we may consider the resolution for elevation angle estimate as the 3-dB beamwidth for comparison with the MIMO case. With this assumption, we can assume that the elevation angle error has a uniform probability distribution between -2.55 and $+2.55$ degrees for the mentioned array. Hence, the root mean square error for the conventional case can be assumed as $\sigma_u = \sqrt{(2.55^2/3)} \approx 1.47$ degrees, which is a value independent of SNR. However, from Fig. 5, we see that the potential estimation accuracy with MIMO techniques is well beyond the conventional approach, especially for high SNR values. Studying feasibility of the mentioned theoretical performance improvement is the main purpose of this article. Additionally, it should be noted that by using MIMO techniques, the target position is estimated on the received data without the need of transmitting additional probing signals to different elevation angles to execute a possibly time consuming

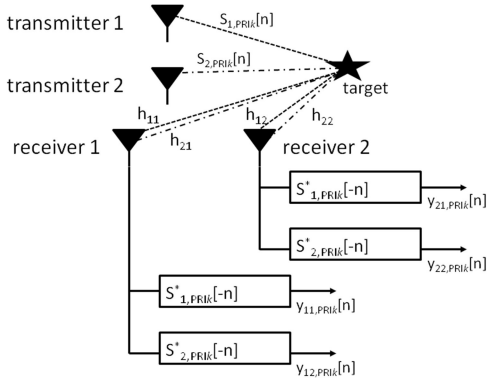


Fig. 6. Space-time coding scheme for two transmit signals at k th PRI, where $k = 1, 2$.

search over a finer grid of transmit beams. Hence, MIMO architecture can also bring some advantages in the beam management/scheduling of the track and search systems.

IV. SPACE-TIME CODING FOR MIMO CONFIGURATION

So far, the transmitted signals are assumed to be perfectly orthogonal, but in practice it is hard to achieve this goal. A highly practical approach to this aim is to divide the available signal bandwidth into several nonoverlapping intervals, possibly with guard intervals in between, and assign unique waveforms covering the spectrum of each interval. This approach clearly satisfies the orthogonality condition at the expense of a reduction in the range resolution of the system. In [24], other approaches, specifically for MIMO sonar systems, are listed as follows.

- 1) Pseudorandom signals generated by filtering white noise through bandpass filters whose frequency spectra are not overlapping.
- 2) FM signals with frequency shifts minimizing cross correlations between each other.
- 3) Binary phase-shift keying modulated Gold sequences.

However, none of the alternatives produce perfectly orthogonal signals as indicated by the orthogonality measures given in [24] which can possibly jeopardize the promised performance improvement described in Section III.

In this article, we evaluate the usage of a space-time coding scheme with complementary codes to achieve the orthogonality requirement of a MIMO sonar system and perform field experiments with the introduced MIMO Mills Cross architecture. In Fig. 6, the concept is illustrated when two different signals are transmitted within two consecutive PRIs. At each receiver there exists a matched filter for each one of the transmitted signals. We will show that by adding each matched filter output throughout the successive PRIs, we obtain the channel response h_{ij} by using complementary codes. This process can be expressed as:

$$h_{ij} \sim \sum_k y_{ji,\text{PRI}_k} \quad (8)$$

where y_{ji,PRI_k} represents the matched filter output as shown in Fig. 6. In [29], the use of complementary codes in a pulse-by-pulse basis for MIMO radar is introduced. By assuming there exists only one target and the Doppler shift is negligible, the system model in [29] can be simplified as

$$\mathbf{R} = \mathbf{H}^T * \mathbf{E} + \mathbf{N}. \quad (9)$$

Here, \mathbf{R} is the receive matrix whose rows represent the receiving antennas, and columns represent the successive PRIs. Similarly, \mathbf{E} is the transmitted signal matrix representing the signals transmitted from each antenna for successive PRIs. \mathbf{N} is the noise matrix and \mathbf{H} is the channel response matrix whose i,j th element h_{ij} represents the channel response from the i th transmitting antenna to the j th receiving antenna. The $*$ operator in the model defines matrix convolution. We can process the receive matrix with the matched filter, \mathbf{E}^H , as [32]

$$\mathbf{E} * \mathbf{E}^H = \gamma \mathbf{I} \delta[n] \quad (10)$$

where γ is a constant, \mathbf{I} is the identity matrix, and $\delta[n]$ is the delta function. Hence, the observation becomes

$$\mathbf{R} * \mathbf{E}^H = \gamma \mathbf{H}^T + \mathbf{N}'$$

where

$$\mathbf{N}' = \mathbf{N} * \mathbf{E}^H. \quad (11)$$

Hence, the channel responses for each transmit and receive pair is perfectly separated with some noise which is the goal that we are trying to achieve with the MIMO Mills Cross architecture.

At this point, we may consider Golay complementary sequences to achieve the condition given in (10). According to [32], a pair of sequences $e_1[n]$ and $e_2[n]$ of length L are said to be complementary, if

$$R_{e_1 e_1}[l] + R_{e_2 e_2}[l] = \begin{cases} 2L, & \text{if } l = 0 \\ 0, & \text{otherwise.} \end{cases} \quad (12)$$

In (12), $R_{e_i e_i}[l]$ represents the linear convolution of $e_i[l]$ and $e_i^*[-l]$, for $l = -L-1, \dots, L-1$ (i.e., autocorrelation function of $e_i[n]$). With this property in mind, we can define our signal matrix $\mathbf{E}_{2 \times 2}$ as [32]

$$\mathbf{E}_{2 \times 2} = \begin{bmatrix} e_1[n] & -e_2^*[-n] \\ e_2[n] & e_1^*[-n] \end{bmatrix}. \quad (13)$$

In (13), each row of the matrix represents the signal to be transmitted from one sensor. At each PRI, one signal set from the columns of $\mathbf{E}_{2 \times 2}$ is transmitted. For instance, at the first PRI the first transmit subarray emits $e_1[n]$, whereas the second one emits $e_2[n]$. Hence, (13) represents a 2×2 scheme where two complementary signals are transmitted from two different sensors in two consecutive PRIs. Now, with the following $\mathbf{E}_{2 \times 2}^H$ matrix presented in [32], which represents the matched filters on reception, (10) shall be satisfied:

$$\mathbf{E}_{2 \times 2}^H = \begin{bmatrix} e_1^*[-n] & e_2^*[-n] \\ -e_2[n] & e_1[n] \end{bmatrix}. \quad (14)$$

Hence, with the 2×2 scheme we can partition our conventional Mills Cross architecture into two transmit and two receive subarrays to evaluate MIMO radar/sonar concept by using two consecutive transmissions. The matrices in (13) and (14) can be related with the architecture in Fig. 6 as follows:

$$\mathbf{E}_{2 \times 2} = \begin{bmatrix} s_{1,\text{PRI}_1}[n] & s_{1,\text{PRI}_2}[n] \\ s_{2,\text{PRI}_1}[n] & s_{2,\text{PRI}_2}[n] \end{bmatrix}$$

$$\mathbf{E}_{2 \times 2}^H = \begin{bmatrix} s_{1,\text{PRI}_1}^*[-n] & s_{2,\text{PRI}_1}^*[-n] \\ s_{1,\text{PRI}_2}^*[-n] & s_{2,\text{PRI}_2}^*[-n] \end{bmatrix}.$$

If we sum the matched filter outputs as in (8), we obtain the following results after omitting the noise term at the moment

$$\sum_k y_{11,\text{PRI}_k} = (h_{11} * e_1[n] + h_{21} * e_2[n]) * e_1^*[-n]$$

$$+ (h_{11} * (-e_2^*[-n]) + h_{21} * e_1^*[-n]) * (-e_2[n])$$

$$= h_{11} * R_{e_1 e_1}[n] + h_{11} * R_{e_2 e_2}[n]$$

$$= h_{11} * 2L\delta[n]$$

$$\sum_k y_{12,\text{PRI}_k} = (h_{11} * e_1[n] + h_{21} * e_2[n]) * e_2^*[-n]$$

$$+ (h_{11} * (-e_2^*[-n]) + h_{21} * e_1^*[-n]) * e_1[n]$$

$$= h_{21} * R_{e_1 e_1}[n] + h_{21} * R_{e_2 e_2}[n]$$

$$= h_{21} * 2L\delta[n]$$

$$\sum_k y_{21,\text{PRI}_k} = (h_{12} * e_1[n] + h_{22} * e_2[n]) * e_1^*[-n]$$

$$+ (h_{12} * (-e_2^*[-n]) + h_{22} * e_1^*[-n]) * (-e_2[n])$$

$$= h_{12} * R_{e_1 e_1}[n] + h_{12} * R_{e_2 e_2}[n]$$

$$= h_{12} * 2L\delta[n]$$

$$\sum_k y_{22,\text{PRI}_k} = (h_{12} * e_1[n] + h_{22} * e_2[n]) * e_2^*[-n]$$

$$+ (h_{12} * (-e_2^*[-n]) + h_{22} * e_1^*[-n]) * e_1[n]$$

$$= h_{22} * R_{e_1 e_1}[n] + h_{22} * R_{e_2 e_2}[n]$$

$$= h_{22} * 2L\delta[n].$$

Hence, we can obtain the channel response matrix \mathbf{H} as in (8). Now, let us inject white Gaussian noise $w_1[n]$ and $w_2[n]$ from receiver-1 and receiver-2, respectively. The autocorrelation functions of $w_1[n]$ and $w_2[n]$ are

$$R_{w_1 w_1}[n] = R_{w_2 w_2}[n] = \delta[n]$$

since $w_1[n]$ and $w_2[n]$ are white. The autocorrelation functions of the noise components after matched filtering can be defined as $R_{w_{ij} w_{ij},\text{PRI}_k}[n]$ representing the i th noise signal at the output of the j th matched filter at PRI_k . If we sum the noise signals at each matched filter output throughout the successive PRIs in a similar fashion as described with the previous derivations, the autocorrelation functions become

$$R_{w_{ij} w_{ij},\text{PRI}_1}[n] + R_{w_{ij} w_{ij},\text{PRI}_2}[n]$$

$$= \delta[n] * R_{e_1 e_1}[n] + \delta[n] * R_{e_2 e_2}[n] = 2L\delta[n].$$

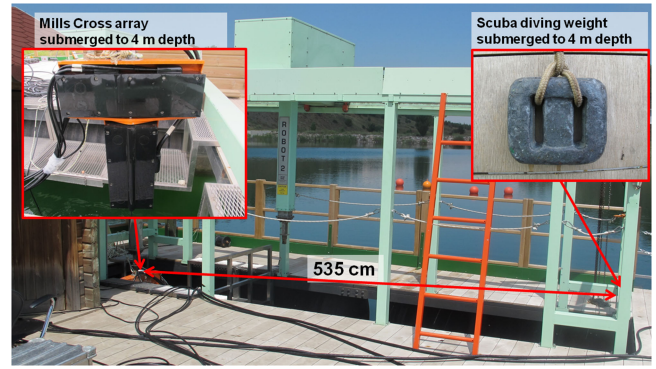


Fig. 7. Test setup at Yalincak Dam.

Therefore, we can state that after adding the matched filter outputs throughout successive PRIs we obtain again additive white Gaussian noise with the signal components. In other words, \mathbf{N}' in (11) is again white Gaussian noise matrix if \mathbf{N} in (9) represents additive independent identically distributed white Gaussian noise.

In [29], the 2×2 scheme presented so far, is further extended to a 4×4 scheme. It is proven that if the conditions given in [29] are satisfied, perfect separation between channel responses can be achieved with four subarrays in four consecutive PRIs. In the next section, we present the results of a field test to evaluate the performance of a practical MIMO Mills Cross system space-time coded with the complementary sequences.

V. FIELD TESTS

A. Experiment Setup and System Parameters

The test hardware is based on an active sonar system for mine and obstacle avoidance using a Mills Cross type sensor array. After some modifications on the original system, the 2×2 scheme using complementary codes was developed. The test system includes a transmitter array composed of two 10-element subarrays and a receiving array composed of 24 elements. Since the main purpose of the experiment is estimating the elevation angle, the receiver array was not partitioned into smaller subarrays. The test is conducted in the facilities located at Yalincak Dam, Middle East Technical University, Ankara shown in Fig. 7. The sensor array was positioned at approximately 4 m depth. Target was positioned 535 cm away from the boresight of the array (at the same depth of 4 m) as illustrated in Fig. 8. The target used for the tests was a scuba diving weight, shown in Fig. 8, with the dimensions of approximately 9×10 cm.

For the elevation angle measurements, the following binary Golay complementary codewords

$$e_1[n] = \begin{bmatrix} 1 & 1 & 1 & -1 & 1 & 1 & -1 & 1 \end{bmatrix}$$

$$e_2[n] = \begin{bmatrix} 1 & 1 & 1 & -1 & -1 & -1 & 1 & -1 \end{bmatrix}$$

were transmitted in two consecutive PRIs according to the signal matrix $\mathbf{E}_{2 \times 2}$ in (13). The chip duration of 0.1 ms,

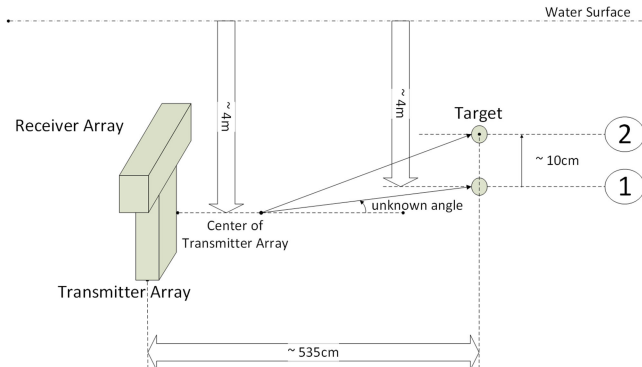


Fig. 8. Geometry of the test setup.

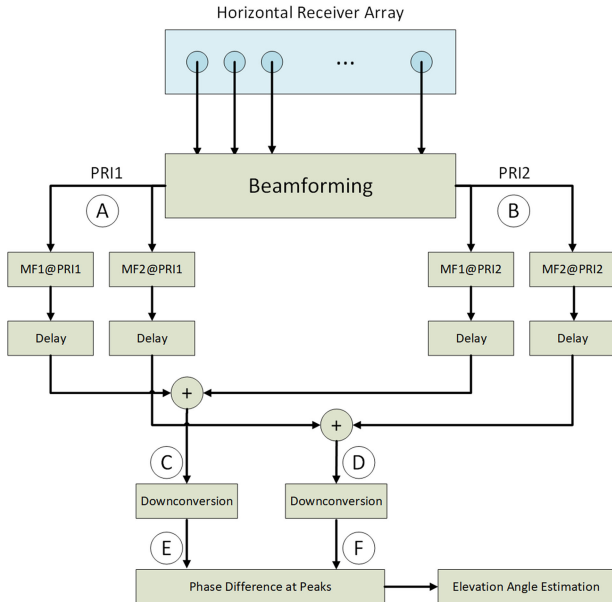


Fig. 9. Block diagram of the elevation angle estimation procedure.

the carrier frequency of 80 kHz, and the sampling rate of 400 kHz are other system parameters.

B. Elevation Angle Estimation by Relative Position Change

Both the sensor array and target were positioned at 4 m depth, approximately. The positioning is not exact due to the uncontrolled environmental effects such as surface wave and current conditions. First, the initial target position was estimated with the proposed architecture. Then, the target was lifted by 10 cm in the upwards direction, i.e., moved from position 1 to position 2 in Fig. 8. The measurements were repeated for the new position to evaluate if the relative change in target position was estimated correctly by the MIMO system or not. The procedure used for the elevation angle estimation is outlined as a block diagram in Fig. 9.

1) *Demonstration of Achieved Orthogonality:* The received echoes at each receiving sensor were combined to obtain the beamformed data for each PRI. The beamformer outputs for the first and second PRIs are shown in Figs. 10 and 11 for a typical measurement. These figures indicate the

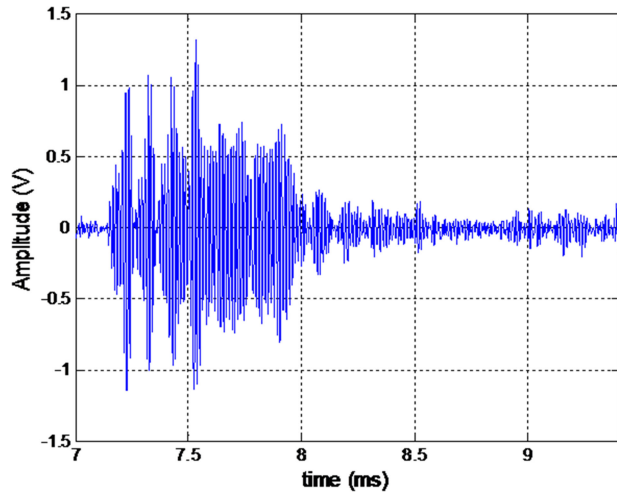


Fig. 10. Beamformer output of the target echo signal at the first PRI (time domain signal at point A of Fig. 9). The horizontal axis represents the time lapsed from the beginning of the transmitted pulse.

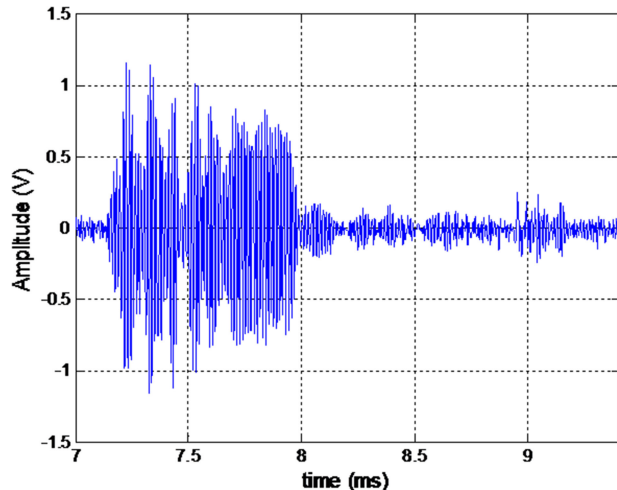


Fig. 11. Beamformer output of the target echo signal at the second PRI (time domain signal at point B of Fig. 9). The horizontal axis represents the time lapsed from the beginning of the transmitted pulse.

typical signal at the points A and B of the processing chain shown in Fig. 9. Next, the time domain signal was filtered with the corresponding matched filters. Then, the matched filter outputs of the first and second PRIs were summed up. The summation of the matched filter outputs (signals at the points C and D of the processing chain) is shown in Fig. 12.

From Figs. 10 and 11, we observe that the transmitted pulses (complementary codes) of duration 0.8 ms is received with some multipath effects at both PRIs. Once operations of the matched filtering and summation of matched filters for different PRIs are implemented, the resulting signal duration significantly reduces indicating the cancellation effect due to the complementary nature of the codes. Furthermore, the magnitude of the baseband signals after downconversion (signals at points E and F of the processing chain) is also shown in Fig. 13. From these figures, we can note that the final output gets closer to the ideal delta function as the signal processed through the chain. The

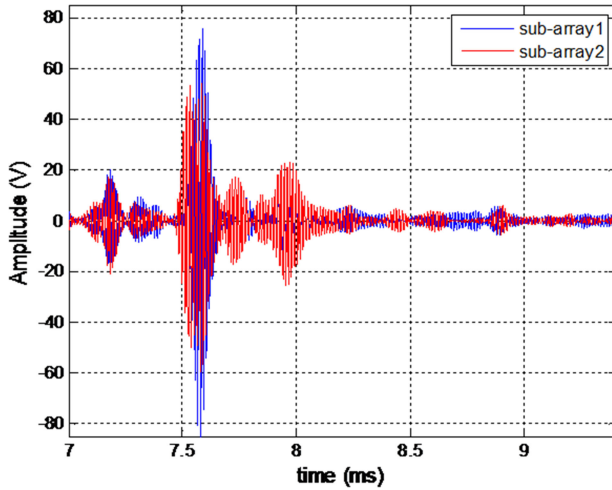


Fig. 12. Sum of matched filter outputs of subarray1 and subarray2 (time domain signals at C and D in Fig. 9, respectively).

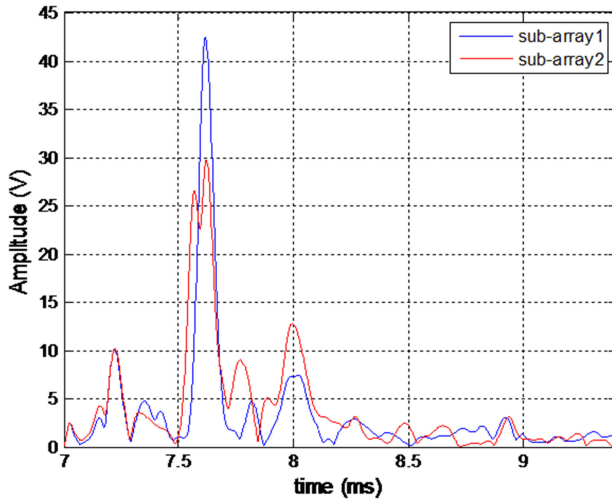


Fig. 13. Magnitudes of the sum of matched filter outputs of subarray1 and subarray2 in baseband (time domain signals at E and F in Fig. 9, respectively).

TABLE II
Statistics of the Measurements of the First Test

Target Position	Average SNR (dB)	Mean of Elevation Estimate (degrees)	Standard Deviation of Elevation Estimate (degrees)	Estimated Depth (cm)
1	49	90.761	0.090	392.9
2	49	91.820	0.047	383.0

side-lobes observed in Fig. 13 can be explained by the imperfections of the setup and also a possible motion of the target between two PRIs.

2) *Statistical Evaluation of Estimation Accuracy:* 100 successive measurements were made for each position and the statistics of the results are summarized in Table II. The main conclusion that we can derive from Table II is, when the target is moved by 10 cm upwards (from position 1 to position 2 as shown in Fig. 8) this change in target depth at 535 cm distance is estimated as

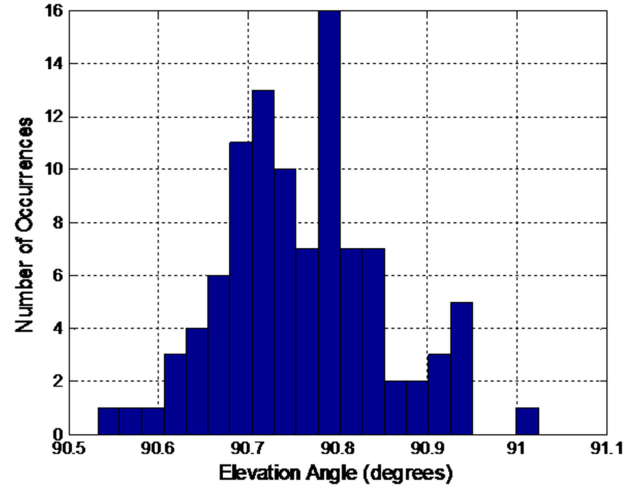


Fig. 14. Histogram of elevation angle measurements at position 1.

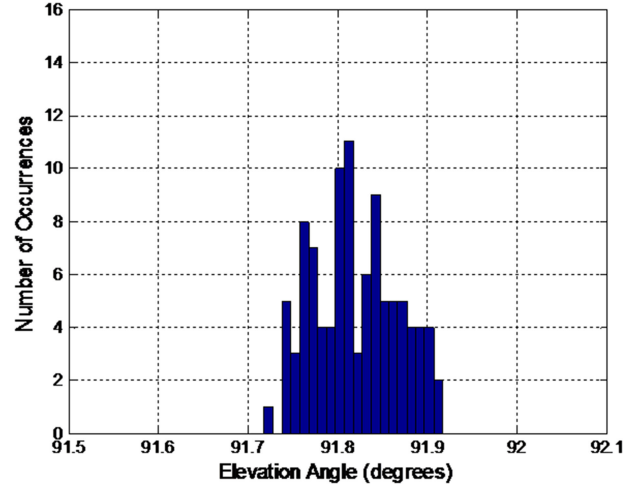


Fig. 15. Histogram of elevation angle measurements at position 2.

392.9–383.0 = 9.9 cm which is consistent with the test setup within positioning errors. The histograms of the calculated elevation angles for each position are shown in Figs. 14 and 15. The average SNR for the measurements were calculated on the summations of the matched filter outputs of two successive receptions. The peak values of the matched filters after summation were considered to calculate the average signal power. The noise power was calculated within a small window where the echo signals were minimum at each PRI, and the average noise power value was used to obtain the SNR values.

3) *Performance Evaluation With Additive Synthetic Noise:* According to the SNR calculations, the ambient noise power at Yalincak Dam is very low. Synthetic noise was added to the summation of the matched filter outputs of one of the real measurements to evaluate the performance under higher noise conditions. For this purpose, Gaussian noise with zero mean was used and the variance of the noise signal was varied to obtain different SNR values with 1 dB steps. The mean value and the standard deviation of the elevation angle estimates with respect to SNR are shown in Figs. 16 and 17, respectively.

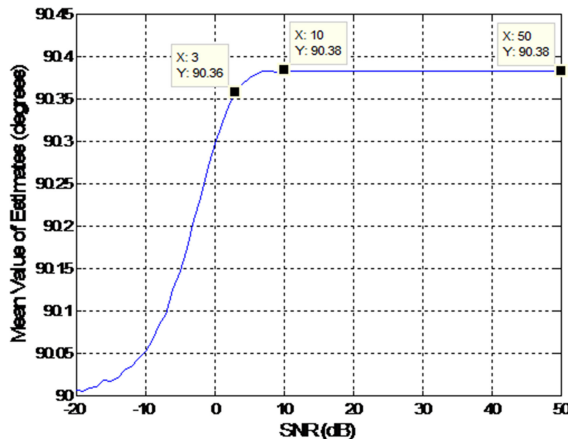


Fig. 16. Mean value of the elevation angle estimates versus SNR.

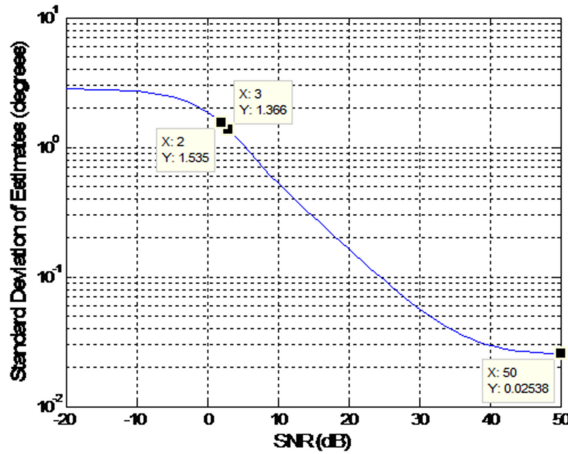


Fig. 17. Standard deviation of the elevation angle estimates versus SNR.

C. Comments on the Test Results

According to the CRLB calculations in Section III, the standard deviation of the error can be reduced to the order of 10^{-3} degrees with the SNR values calculated for the tests, but the resulting standard deviations of the elevation estimate are significantly higher. Throughout the tests, as SNR increases there was no significant improvement on the elevation angle estimation error. We conclude that the limiting factor on the elevation estimation error is the unmodeled effects such as the slight motion of the target between the measurements and interference effects. When we inject synthetic noise to one of the measurements, according to the Figs. 16 and 17, the performance degrades for SNR values less than 3 dB. However, for SNR values greater than 3 dB, we obtain better performance when considering the standard deviation of the conventional case which is 1.47 degrees.

We can conclude that the elevation angle estimation with the proposed MIMO techniques has an accuracy that cannot be achieved by the conventional Mills Cross structure provided that SNR is sufficiently high. A conventional structure with the parameters matching the field test setup has a 3-dB beamwidth of 5.1 degrees. For the target localization experiments mentioned so far, the conventional system cannot

discriminate the displacement of the target and would point at the same elevation location at all experiments.

VI. CONCLUSION

The motivation behind this work is mainly to use MIMO techniques with a Mills Cross architecture to achieve higher accuracy in DOA angle estimation along the dimension on which the transmitter array extends. To achieve the theoretical performance gains of the MIMO system, Golay complementary codes are used at successive PRIs. When the target position in elevation is roughly determined by conventional methods, the procedure introduced in this work can be applied to achieve an accurate elevation angle estimation. If a conventional Mills Cross sonar system is capable of transmitting independent signals concurrently, the MIMO mode can be implemented as an additional capability for the system. For the success of the MIMO mode, when using complementary codes in successive PRIs, the main assumption is the stationarity of the channel. In other words, we assume that the positions of the sensor array and the target along with the underwater conditions remain the same during the consecutive PRIs. This assumption can also be satisfied when the relative displacement of sensor or target is negligible. Detection of mines and other obstacles with a slowly moving platform in short ranges suits well to this scenario.

ACKNOWLEDGMENT

This study was conducted during the employment of the first author at SST-ASELSAN, Inc. Ankara, Turkey. The authors would like to thank S. Özgün (director of Design Engineering of SST-ASELSAN, Inc. at the time of writing), S. Avşar and K. Kürekli (managers of Underwater Acoustical Systems Department and Digital and Embedded Systems Electronic Hardware Design Department of SST-ASELSAN, Inc. at the time of writing) for their support throughout this work. The authors would also like to thank A. Şahin, A. Beder, M. Göçer, T. Bahadir Sarıkaya, M. Can Akpulat, İ Yazgı, and O. Ulaş Şahin (colleagues at SST-ASELSAN, Inc. at the time of writing) for their invaluable help and support to realize the practical evaluation of the concept.

REFERENCES

- [1] B. Y. Mills and A. G. Little
A high resolution aerial system of a new type
Australian J. Phys., vol. 6, pp. 272–278, 1953.
- [2] R. J. Urick
Principles of Underwater Sound, 3rd ed. Los Altos, CA, USA: Peninsula, 1983.
- [3] R. H. MacPhie
A mills cross multiplicative array with the power pattern of a conventional planar array
In Proc. IEEE Antennas Propag. Soc. Int. Symp., Jun. 2007, pp. 5961–5964.
- [4] *Multibeam Sonar Theory of Operation*, L3 Communications SeaBeam Instruments, 2000. [Online]. Available: <http://www.mbari.org/data/mbsystem/sonarfunction/SeaBeamMultibeamTheoryOperation.pdf>

- [5] EM 302 30 kHz Multibeam Echo Sounder, Kongsberg Maritime AS, 2013. [Online]. Available: [http://www.km.kongsberg.com/ks/web/nokbg0397.nsf/AllWeb/A915A71E90B6CFAEC12571B1003FE84D/\\$file/306106_em302_product_specification.pdf?OpenElement](http://www.km.kongsberg.com/ks/web/nokbg0397.nsf/AllWeb/A915A71E90B6CFAEC12571B1003FE84D/$file/306106_em302_product_specification.pdf?OpenElement)
- [6] *SeaBat 7125 Ultra High Resolution Multibeam Echo Sounder*, Teledyne RESON A/S, 2015. [Online]. Available: http://www.teledyne-reson.com/download/Seabat_product_leaflet/SeaBat%207125%20product%20leaflet%20pld137777-12.pdf
- [7] M. Meister and G. Zindel
Safe navigation in hazardous areas: forward-looking sonar for submarines
Sea Technol., vol. 53, no. 11, pp. 21–27, Nov. 2012. [Online]. Available: www.sea-technology.com
- [8] C. Degel *et al.*
3D sonar system based on mills cross antenna configuration
In *Proc. OCEANS*, Sep. 2014, pp. 1–6.
- [9] A. M. Haimovich, R. S. Blum, and L. J. Cimini
MIMO radar with widely separated antennas
IEEE Signal Process. Mag., vol. 25, no. 1, pp. 116–129, Jan. 2008.
- [10] K. W. Forsythe and D. W. Bliss
MIMO radar: Concepts, performance enhancements, and applications
In *MIMO Radar Signal Processing*, J. Li and P. Stoica, Eds. Hoboken, NJ, USA: Wiley, 2009, pp. 65–121.
- [11] B. Friedlander
Adaptive signal design for MIMO radars
In *MIMO Radar Signal Processing*, J. Li and P. Stoica, Eds. Hoboken, NJ, USA: Wiley, 2009, pp. 193–235.
- [12] Y. Pailhas, Y. Petillot, C. Capus, and B. Mulgrew
Target detection using statistical MIMO
In *Proc. Meetings Acoust. Acoustical Soc. Amer.*, vol. 17, no. 1, pp. 1716–1722, 2012.
- [13] J. Yong and C. Guoqiang
Long distance target DOA estimation by MIMO sonar
In *Proc. Int. Conf. Artif. Intell. Comput. Intell.*, Oct. 2010, vol. 2, pp. 111–114.
- [14] C. Sun, X. Liu, J. Zhuo, and Z. Liu
High-resolution 2-D sector-scan imaging using MIMO sonar with narrowband LFM pulses
In *Proc. OCEANS*, Sep. 2013, pp. 1–5.
- [15] N. Sharaga and J. Tabrikian
Optimal adaptive transmit beamforming for cognitive MIMO sonar in a shallow water waveguide
In *Proc. 22nd Eur. Signal Process. Conf.*, Sep. 2014, pp. 1960–1964.
- [16] Y. Pailhas and Y. Petillot
MIMO sonar systems for harbour surveillance
In *Proc. OCEANS*, May 2015, pp. 1–6.
- [17] M. Jiang, J. Huang, W. Han, and F. Chu
Research on target DOA estimation method using MIMO sonar
In *Proc. 4th IEEE Conf. Ind. Electron. Appl.*, May 2009, pp. 1982–1984.
- [18] J. Huang, L. Zhang, Q. Zhang, Y. Jin, and M. Jiang
Performance analysis of DOA estimation for MIMO sonar based on experiments
In *Proc. IEEE/SP 15th Workshop Statist. Signal Process.*, Sep. 2009, pp. 269–272.
- [19] I. Bekkerman and J. Tabrikian
Target detection and localization using MIMO radars and sonars
IEEE Trans. Signal Process., vol. 54, no. 10, pp. 3873–3883, Oct. 2006.
- [20] H. Li and B. Himed
Transmit subaperturing for MIMO radars with co-located antennas
IEEE J. Sel. Topics Signal Process., vol. 4, no. 1, pp. 55–65, Feb. 2010.
- [21] D. R. Fuhrmann, J. P. Browning, and M. Rangaswamy
Signaling strategies for the hybrid MIMO phased-array radar
IEEE J. Sel. Topics Signal Process., vol. 4, no. 1, pp. 66–78, Feb. 2010.
- [22] A. Hassanien and S. A. Vorobyov
Phased-MIMO radar: A tradeoff between phased-array and MIMO radars
IEEE Trans. Signal Process., vol. 58, no. 6, pp. 3137–3151, Jun. 2010.
- [23] L. Cai, X. Ma, and S. Li
On orthogonal waveform design for MIMO sonar
In *Proc. Int. Conf. Intell. Control Inf. Process.*, Aug. 2010, pp. 69–72.
- [24] S. Wentao, H. Jianguo, C. Xiaodong, and H. Yunshan
Orthogonal waveforms design and performance analysis for MIMO sonar
In *Proc. IEEE 10th Int. Conf. Signal Process.*, Aug. 2010, pp. 2382–2385.
- [25] S. D. Blunt and E. L. Mokole
Overview of radar waveform diversity
IEEE Aerosp. Electron. Syst. Mag., vol. 31, no. 11, pp. 2–42, Nov. 2016.
- [26] M. Golay
Complementary series
IRE Trans. Inf. Theory, vol. 7, no. 2, pp. 82–87, Apr. 1961.
- [27] S. Y. Sun, H. H. Chen, and W. X. Meng
A survey on complementary-coded MIMO CDMA wireless communications
IEEE Commun. Surv. Tuts., vol. 17, no. 1, pp. 52–69, Jan.–Mar. 2015.
- [28] N. Levanon, I. Cohen, and P. Itkin
Complementary pair radar waveforms-evaluating and mitigating some drawbacks
IEEE Aerosp. Electron. Syst. Mag., vol. 32, no. 3, pp. 40–50, Mar. 2017.
- [29] T. R. Qureshi, M. D. Zoltowski, R. Calderbank, and A. Pezeshki
Unitary design of radar waveform diversity sets
Digit. Signal Process., vol. 21, no. 5, pp. 552–567, Sep. 2011.
- [30] S. M. Kay
Fundamentals of Statistical Signal Processing. Vol 1, Estimation Theory. Englewood Cliffs, NJ, USA: Prentice-Hall, 1993.
- [31] M. A. Richards
Fundamentals of Radar Signal Processing, 2nd ed. New York, NY, USA: McGraw-Hill, 2014.
- [32] T. Qureshi, M. Zoltowski, and R. Calderbank
MIMO-OFDM channel estimation using Golay complementary sequences
In *Proc. Int. Waveform Diversity Des. Conf.*, Feb. 2009, pp. 253–257.



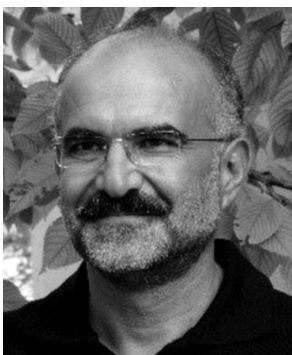
Cahit Uğur Üngan received the B.S. and M.S. degrees in electrical and electronics engineering from Middle East Technical University, Ankara, Turkey, in 2002 and 2005, respectively. He is currently working toward the Ph.D. degree in electrical and electronics engineering with the Middle East Technical University, Ankara, Turkey.

Since 2002, he has been a Digital Design Engineer with ASELSAN, Inc., Ankara, Turkey, where he has been working on underwater acoustics related projects, which require collaboration between industry and academia for more than five years.



Çağatay Candan received the B.S. degree from Middle East Technical University, Ankara, Turkey, in 1996, the M.S. degree from Bilkent University, Ankara, Turkey, in 1998, and the Ph.D. degree from the Georgia Institute of Technology, Atlanta, GA, USA, in 2004, all in electrical engineering.

He is currently a Professor with the Department of Electrical and Electronics Engineering, Middle East Technical University, Ankara, Turkey. His research interests are statistical signal processing and its applications.



Tolga Ciloglu received the B.S., M.S., and Ph.D. degrees in electrical and electronics engineering from Middle East Technical University, Ankara, Turkey, in 1985, 1987, and 1994, respectively.

He is currently a Professor with the Department of Electrical and Electronics Engineering, Middle East Technical University, Ankara, Turkey. His research interests are statistical signal processing, and speech and audio processing.